

NPS ARCHIVE
1959
THOMAS, P.

AN ANECHOIC TANK FOR UNDERWATER
SOUND STUDIES AND INVESTIGATION
OF SOUND PRESSURE FIELDS
IN A TWO-LAYER MODEL

PAUL B. THOMAS
AND
ORVAL K. HALLAM

LIBRARY
U.S. NAVAL POSTGRADUATE SCHOOL
MONTEREY, CALIFORNIA

'851.

AN ANECHOIC TANK FOR UNDERWATER SOUND STUDIES
AND INVESTIGATION OF SOUND PRESSURE
FIELDS IN A TWO-LAYER MODEL

* * * * *

Paul B. Thomas
and
Orval K. Hallam

AN ANECHOIC TANK FOR UNDERWATER SOUND STUDIES
AND INVESTIGATION OF SOUND PRESSURE
FIELDS IN A TWO-LAYER MODEL

by

Paul B. Thomas

Lieutenant Commander, United States Navy

and

Orval K. Hallam

Lieutenant Commander, United States Navy

Submitted in partial fulfillment of
the requirements for the degree of

MASTER OF SCIENCE

United States Naval Postgraduate School
Monterey, California

1959

NPS Archive

1959

Thomas, P.

~~Thesis~~

~~CONFIDENTIAL~~

~~142~~

~~50~~

~~CONFIDENTIAL~~

~~CONFIDENTIAL~~

~~50~~

~~CONFIDENTIAL~~

AN ANECHOIC TANK FOR UNDERWATER SOUND STUDIES
AND INVESTIGATION OF SOUND PRESSURE
FIELDS IN A TWO-LAYER MODEL

by

Paul B. Thomas

and

Orval K. Hallam

This work is accepted as fulfilling
the thesis requirements for the degree of
MASTER OF SCIENCE

from the

United States Naval Postgraduate School

ABSTRACT

The prediction of sound transmission in shallow water is a complex problem. Theoretical solutions exist for ideal situations which seldom exist in nature. An approach to the solution of non-ideal cases is through modeling studies. This paper is divided into two major sections; the first describes the preparation of an anechoic test tank for modeling studies. The second section describes the results of experimentation in a two-layer liquid model.

The writers wish to express their appreciation for the assistance and encouragement given them by Dr. Herman Medwin of the U. S. Naval Postgraduate School in this study.

TABLE OF CONTENTS

Section	Title	Page
1.	Introduction	1
2.	Theory	2
3.	Equipment	5
4.	Tank-Testing Procedures	8
5.	Two-layer Model	10
6.	Conclusions	13
7.	Recommendations	14
8.	Bibliography	28

LIST OF ILLUSTRATIONS

Figure		Page
1.	Diagram of Relative Positions of Source, Receiver and Image	15
2.	Photograph of Tank and Associated Equipment	16
3.	Isometric Drawing of Sound Absorbing Wedge	17
4.	Photograph of Sound Source and Receiver	18
5.	Diagram of Sound Source Electronic Equipment	19
6.	Block Diagram of Sound Receiver and Recorder Electronic Equipment	20
7.	Sound Pressure Patterns Showing Drop-off from R_c to $3 R_c$	21
8.	Sound Pressure Patterns Showing Effect of Extremes in Source and Receiver Depths	22
9.	Sound Pressure Patterns with Product of h and d a Constant	23
10.	Vertical Sound Pressure Patterns from Surface to Source in the Two-Layer Model	24
11.	Sound Pressure Patterns Along the Bottom of the Oil Layer at Various Source Depths " d ." Layer Depth 11.4 cm.	25
12.	Sound Pressure Patterns Along the Bottom of the Oil Layer at Various Source Depths " d ." Layer Depth 9.6 cm.	26
13.	Sound Pressure Patterns Along the Bottom of the Oil Layer at Different Source Depths " d ." Layer Depth 7.5 cm.	27

1. Introduction

The prediction of sound transmission in shallow water is a complex problem which has been studied for many years. A theoretical solution to the problem was presented by Pekeris [1]. The Pekeris solution, known as the liquid bottom solution, is restricted to bottom materials which cannot sustain shear waves. Weinstein [2] obtained experimental verification of the Pekeris solution for a liquid bottom and extended the solution to a bottom which could sustain shear waves. The experiments performed by Weinstein provide conclusive proof that the existing theory is correct for ideal cases in which the bottom is level and uniform and its acoustic properties known. However, these ideal cases are seldom found in nature. As a result, in spite of previous work done on the problem, there is no known method which can be used to predict the shallow water transmission of sound when the bottom is irregular and its acoustic properties unknown.

This paper describes the preparation of an anechoic tank which can be used for model studies of sound transmission. Although it was appreciated that such studies could not produce a general solution, further investigation of ideal cases could contribute to our knowledge of the problem. In particular, it is possible that there is a correlation between vertical sound pressure fields and horizontal transmission of sound. Section 5 describes a preliminary attempt at finding this correlation for a simple two-layer model.

2. Theory

A tank used for sound transmission studies must be lined with an absorbing material which will reduce reflected sound waves to an acceptable magnitude. Tank testing methods used in the past are discussed by Yingling and Medwin [3]. It is believed that the Lloyd Mirror test is one of the best methods for use with continuous-wave sound.

The sound pressure detected by a receiver at any point beneath the surface of a semi-infinite medium has two components. The first component is the pressure due to the sound wave which followed a direct path from the source to the receiver; the second component is the pressure due to the sound wave which was reflected from the surface in the direction of the receiver. Since the surface is a pressure-release boundary, this reflected wave is reversed in phase. The geometry may be simplified by considering this out-of-phase component as originating from an image located above the surface at a distance equal to the depth of the source. Fig. 1 shows the relative positions of source, image and receiver.

The net pressure at a receiver at depth h due to an assumed point source at depth d is

$$(1) \quad \underline{p} = \underline{B} e^{j\omega t} \left[\frac{e^{-jk r_1}}{r_1} - \frac{e^{-jk r_2}}{r_2} \right]$$

where: r_1 = distance from source to receiver

r_2 = distance from image to receiver

$$k = \omega/c = 2\pi/\lambda$$

$$\text{expanding } r_2^2 = r^2 + (h+d)^2$$

$$r_2 = r \left[1 + \left(\frac{h+d}{r} \right)^2 \right]^{1/2}$$

$$\text{for } r > h+d$$

$$(2) \quad r_2 \approx r \left[1 + \frac{1}{2} \left(\frac{h+d}{r} \right)^2 \right]$$

similarly

$$(3) \quad r_1 \approx r \left[1 + \frac{1}{2} \left(\frac{h-d}{r} \right)^2 \right]$$

The application of the following simplified equations, which include the above approximations, will be restricted to ranges where

$\frac{h+d}{r} \lesssim 0.4$. The range where $\frac{h+d}{r} = 0.4$ is defined as the minimum range, R_{min}

Substituting (2) and (3) in (1) and simplifying:

$$\underline{p} = \frac{2jB}{r} \left(\sin \frac{kh d}{r} \right) e^{j(\omega t - kr)}$$

The amplitude is

$$(4) \quad P = \frac{2B}{r} \sin \frac{kh d}{r}$$

It is apparent from this equation that there will be a series of maxima and minima, the last maximum occurring at

$$\frac{kh d}{r} = \frac{\pi}{2}$$

This range is defined as the critical range or the Lloyd range, R_c .

$$R_c = \frac{kh d}{\pi/2} = \frac{4hd}{\lambda}$$

Using the sound pressure level at R_c as a reference, the sound pressure level at $r=2R_c$ will be -9.0 db; at $r=3R_c$ the sound pressure level will be -15.5 db. At the range $r=3R_c$ the sine term in equation (4) may be replaced by its argument $\frac{kh d}{r}$, and the pressure amplitude expression simplifies to

$$(5) \quad P = \frac{2B k h d}{r^2}$$

Equation (5) indicates that beyond the range $r=3R_c$ the sound

pressure level decreases at the rate of 12 db per double distance.

This Lloyd mirror effect can be used as a criterion for an anechoic tank. If the tank is to represent a semi-infinite medium, the observed sound pressure field should be in close agreement with that predicted by the above theory. In addition, standing waves present in the tank will be recognized by the half-wave length modulation in the sound pressure level versus range plot.

3. Equipment

An overall view of the test tank and associated equipment is shown in Fig. 2. The tank is six feet long, four feet wide, and two and one-half feet high. To obtain a volume of water which acoustically extends to infinity horizontally and vertically downward, the tank was lined with 'Insulcrete' sound absorbing wedges. These wedges were made of four parts by volume pine sawdust and one part Portland cement - the same as those used by Darner [4]. They have a density of 1.1 grams/cm³ when dry and 1.4 grams/cm³ when saturated with water, and have a measured sound velocity of 1.9×10^5 cm/sec. (Richardson p.265 [5].) A sketch of one of the wedges is shown in Fig. 3; the arrangement of the wedges in the tank may be seen in Fig. 2. It is noted that the specific acoustic impedance of the lining wedges is not much greater than the acoustic impedance of water. Sound waves passing from the water into the wedges encounter a region of increasing impedance. Acoustic energy is absorbed, and according to Richardson [5], the reflection should be about 30% at a frequency of 10 kc/sec., 10% at 100 kc/sec. and 1% at 1 mc/sec.

The sound receiver probe was a barium titanate cylinder having a diameter and length of 1/8 inch and a wall thickness of .032 inch. These dimensions are much smaller than the wave-length of the sound at the frequencies used. This probe had an acoustical sensitivity of -127 db (ref. 1 volt/dyne/cm.²).

It was intended to use a cylindrical barium titanate sound source that was 1/4 inch in diameter, 5/16 inch in length and having a wall thickness of .075 inch. However, calculations based on the piezo-electric strain constants as given by Langevin [6] and the sound pressure equation in Kinsler and Frey p.171 [7] indicated that this source would not have sufficient output when used in conjunction with the 1/8 inch cylindrical

receiver and a microphone amplifier which had a maximum amplification of 80 db. The source used was a radially polarized barium titanate sphere one inch in diameter, having a wall thickness of 2mm and a capacitance of $5400\mu\text{f}$. This source had a resonant frequency of over 50 kc/sec. It was mounted in an adjustable bracket near one end of the tank. Fig. 4 is a photograph of the sound source and receiver.

Fig. 5 shows a schematic and block diagram of the electronic circuit employed to drive the barium titanate sound source. With minor modifications this circuit was the same as that used by Weinstein [2]. The small dimensions of the source limited the sound output to a relatively low level. The use of frequencies below the resonant frequency of the sphere further reduced this output. Therefore, to obtain a satisfactory level, it was necessary that care be taken to match the high impedance of the barium titanate with an appropriate driving circuit. The variable inductor in parallel with the capacitances of the source and connecting coaxial cable formed a tuned circuit which could be adjusted for driving frequencies in the range 20 kc to 40 kc. An HVC-3 inductor was substituted for tests below 20 kc. An undistorted voltage output of adequate magnitude (80 to 100 volts), without overheating of the source, was provided by this single-stage amplifier.

Fig. 6 is a block diagram of the equipment used to amplify the output signal from the receiver and record the sound pressure field. The output from the barium titanate receiver was amplified by a Brüel & Kjaer Microphone Amplifier. This amplifier provides up to 80 db amplification in 1 db steps. The use of a short length of low-capacitance coaxial cable made it unnecessary to employ a cathode follower on the traverse system. The SKL Variable electronic filter was cascaded with a band pass of 2kc. This served to eliminate harmonics of the fundamental and noise present

in the tank.

Sound pressure levels were observed on the VTVM and/or oscilloscope and recorded on the Brüel & Kjaer recorder. This recorder is a high-speed instrument which provides an accurate, continuous record of sound pressure levels.

The electronic circuitry proved to be reliable. The signal to noise ratio was greater than 200:1 at the end of the tank (80 cm. from the source). This made it possible to conduct tests under adverse conditions of outside noise.

The general arrangement of the traverse system may also be seen in Fig. 2. This system, in conjunction with a high speed level recorder, was used to obtain a continuous record of the sound pressure field in the horizontal or in the vertical direction. A movable carriage was mounted on a rectangular metal framework, which in turn was supported on the tank top by four rubber vibration dampeners. These dampeners were fitted with leveling adjustment screws which were set to maintain constant receiver depth during horizontal carriage runs. A 1/10 h.p. electric motor was mounted on the carriage. This motor drove the carriage through a fiber spur gear by engaging a gear rack mounted alongside one of the carriage tracks. The receiver probe was attached to a vertical gear rack mounted in the middle of the carriage. For vertical runs the level recorder drove this gear through a flexible drive shaft and spur gear arrangement. For horizontal runs the vertical gear rack was locked to maintain constant receiver depth.

4. Tank Testing Procedures.

The tank was filled with a saturated salt solution (35 grams/100 ml of water), with the subsequent purpose of conducting experiments in multi-layer liquids using salt water as the bottom layer. This solution was made in 20 gallon increments by dissolving the required amount of commercial rock salt in a suitable container of tap water. Vigorous stirring by a large electric mixer accelerated the dissolving process.

The velocity of sound in this medium was determined by the resonant chamber technique using a 5.25 liter glass sphere. The solution was found to have a density of 1.201 gram/cm^3 and a sound velocity of $1.717 \times 10^5 \text{ cm/sec.}$ giving a specific acoustic impedance of $2.06 \times 10^5 \text{ gram/cm}^2 \text{ sec.}$ Three days after filling the tank the sound velocity and density were again measured and were found to have decreased to $1.64 \times 10^5 \text{ cm./sec.}$ and 1.142 gram/cm^3 respectively. This decreased density corresponded to a salinity of 25 grams/100 ml of water. It was therefore believed that the amount of salt representing the difference between 35 gram/100 ml and 25 gram/100 ml of water had recrystallized in the many minute air spaces of the porous wedges lining the tank. One of the wedges was cut open and this was confirmed. Subsequent measurements of sound velocity and density indicated no appreciable change in either.

To determine the optimum source driving frequency for the experiment, sound pressure patterns within the tank were obtained in 1 kc/sec. increments from 10 kc/sec. to 20 kc/sec. and then from 20 kc/sec. to 40 kc/sec. in increments of 5 kc/sec. As expected, the magnitude of the standing waves or reflections in the tank diminished with increasing frequency. To keep the wave-length of the sound much greater than the dimensions of the source and receiver, 30 kc/sec. was determined to be optimum frequency and all subsequent investigations were conducted at this frequency.

Sound pressure patterns were obtained at various combinations of source depth 'd', receiver depth 'h', and distance of source from end of tank. The tank exhibited the best anechoic properties when the source and receiver depths were between 4 cm. and 9 cm. and the source was 30 cm. from the end of the tank. These limitations are due to reflections from the wedges and interference by the source and receiver mounting tubes. The sound pressure patterns in Fig. 7, obtained at 30 kc/sec, show the sound pressure drop-off of approximately 9 db from R_c to $2 R_c$. This is in good agreement with theory. However, the drop-off at ranges less than R_c was in poor agreement with theoretical values.

Fig. 8 shows sound pressure patterns obtained when the source and/or receiver depths are outside the limits mentioned above. There was no appreciable difference in the patterns obtained when the source and receiver depths were varied within the previously mentioned limits and their product kept at a constant value. This is shown in Fig. 9.

Reflections from the end of the tank opposite the source produced large standing waves out to about 15 cm. from the wedges. The useful length of the tank was therefore limited to the field between R_c and 15 cm. from the end of the tank. Within this range the maximum deviation of observed sound pressure levels from those predicted by theory was about 1.5 db.

5. Two-layer Model.

Liquids suitable for underwater sound model studies and their limitations are discussed in Appendix I. A two-layer model consisting of transformer oil over salt water was determined to be the most practical combination for simulating one type of sea bottom.

Numerous sound pressure patterns were obtained in three different layer depths of oil. These were made in an attempt to determine the feasibility of conducting multi-layer modeling studies in a small tank with the ultimate purpose of determining:

1. The degree of correlation, if any, that exists between the horizontal sound pressure field and the vertical sound field directly above the sound source.
2. The effect of source depth on the sound field along the bottom of the upper layer.

The upper 11.4 cm. of salt water was siphoned from the tank upon completion of the tank tests described in the preceeding section and replaced with a like volume of transformer oil (SHELL DIALA AX). This oil had a density of 0.866 gram/cm³. and a measured (by resonant chamber technique) sound velocity of 1.43×10^5 cm/sec. This resulted in an oil to brine specific acoustic impedance ratio of 1:1.51 which corresponds to sea water over a mud or silty fine sand bottom. Three different layer depths of oil were used, viz. 11.4 cm., 9.6 cm. and 7.4 cm. These depths correspond to 2.4, 2.0, and 1.5 wavelengths, respectively, at a frequency of 30 kc/sec. With the sound source on the bottom of the oil layer vertical sound pressure patterns directly above it were obtained for the three different oil depths. These patterns are shown in Fig. 10. In general, they are similar. The sound pressure level nodes occur at very nearly

one-half wavelength intervals from the oil-air interface down to the source. Minor variations are observed in the rate of drop-off of sound pressure levels in the three layer depths of oil.

Sound pressure patterns along the bottom of the 11.4 cm. oil layer with the center of the source at depths of 10 cm., 5 cm. and 3.5 cm., are shown in Fig. 11. In all three layers there is a rapid drop-off in pressure with distance from the source (approximately 1 db/cm.) out to a range of about $3\frac{3}{4}$ times the layer depth. This is followed by an increase in pressure level and then either a leveling off or a decrease again. In the case of the 7.4 cm. layer, it reaches a peak at a range of about six times the layer depth and then decreases again. The tank is too short to determine whether this same pattern in terms of layer depth occurs in the case of the 9.6 cm. and the 11.4 cm. layers. In general, it is to be expected that the sound pressure level within the shallower layer would be higher than in deeper layers. That this is not observed throughout the patterns may lend further evidence to the belief that at source and receiver depths greater than nine centimeters there was 'pick up' of reflections from the bottom of the tank even though the oil-brine interface will reduce them somewhat.

Figure 12 shows the sound patterns along the bottom obtained in an oil depth of 9.6 cm. with the center of the source at depths of 8 cm., 5 cm. and 3.5 cm.

Figure 13 shows the sound patterns obtained in an oil depth of 7.4 cm. with the center of the source at depths of 6 cm. and 3.5 cm.

There were noticeable differences in the patterns obtained by varying source depth in a given layer depth of oil. With the exception of the 11.4 cm. layer, the propagation appears to be better at a source depth of 3.5 cm.

($3/4$ wave-length). In any case propagation appeared to be poorest when the source is on the bottom of the oil layer.

6. Conclusions.

The tank is essentially anechoic at a frequency of 30 kc/sec when the source and receiver depths are between four and nine centimeters and the observations are restricted to the range from R_c to a point about 15 centimeters from the end of the tank.

There were no significant differences observed in the vertical sound pressure patterns. However, because of the limited data available, it is not possible to arrive at a general conclusion regarding this similarity.

The horizontal propagation of sound was affected by the source depth. However, due to the limited effective length and depth of the tank, it was not possible to determine the significance of the observed variations.

It is deemed feasible to conduct model studies to determine the optimum source depth for best horizontal propagation and the degree of correlation that exists between the vertical and horizontal sound pressure patterns.



7. Recommendations.

It is recommended that further studies be conducted after consideration of the following modifications to the equipment:

1. Increase tank size by at least 50% in each dimension.
2. Use tank lining material that has a higher degree of sound absorption and is preferably non-absorbent to the media in the tank.
3. Decrease the size of the sound source. It should be possible to use a 1/2" diameter sphere if receiver amplification is increased.

These modifications will increase the effective length of the tank, permit use of more realistic source depths, decrease the ratio of source diameter to layer depth and eliminate contamination of absorbing wedges by the fluids.

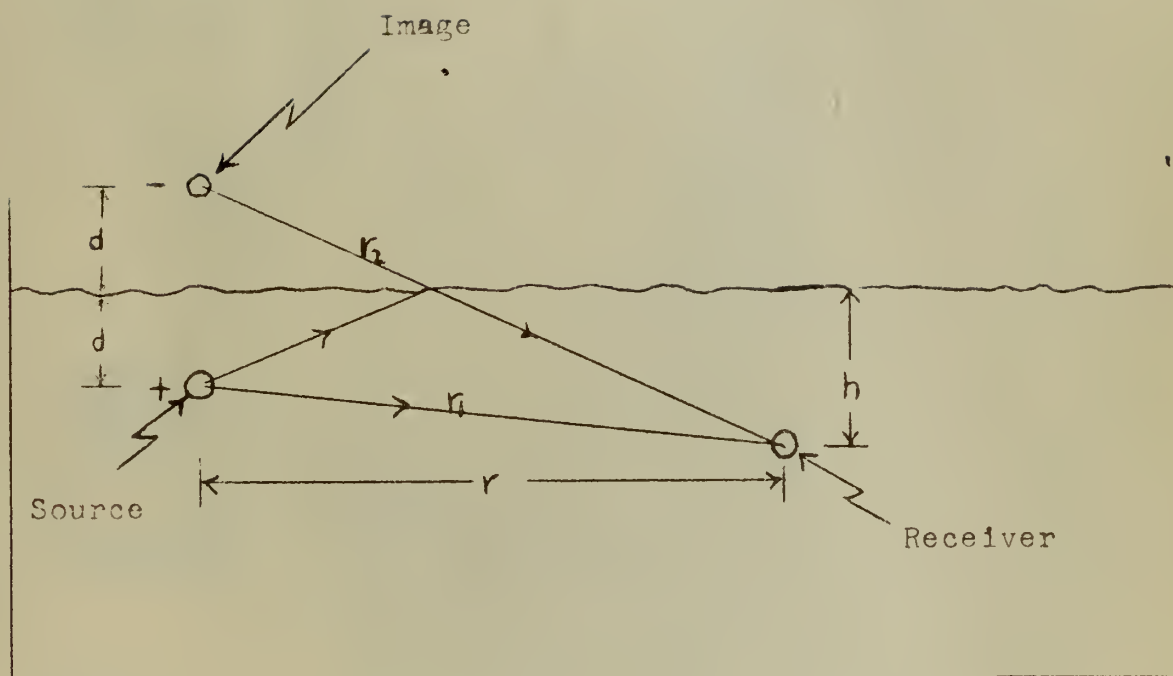


Figure 1 - Relative Positions of Source, Receiver and Image

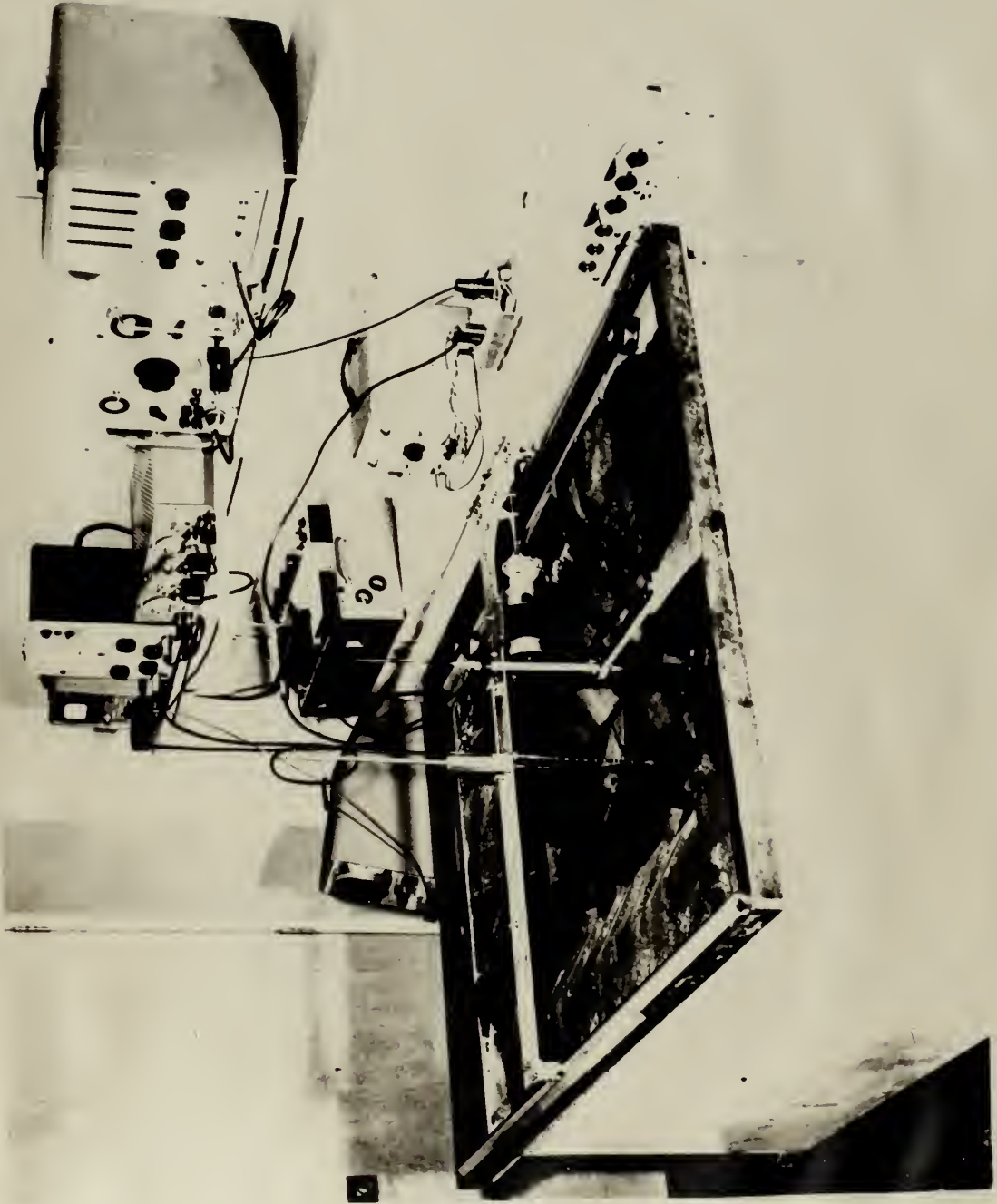


FIGURE 2. TEST TANK AND ASSOCIATED EQUIPMENT.

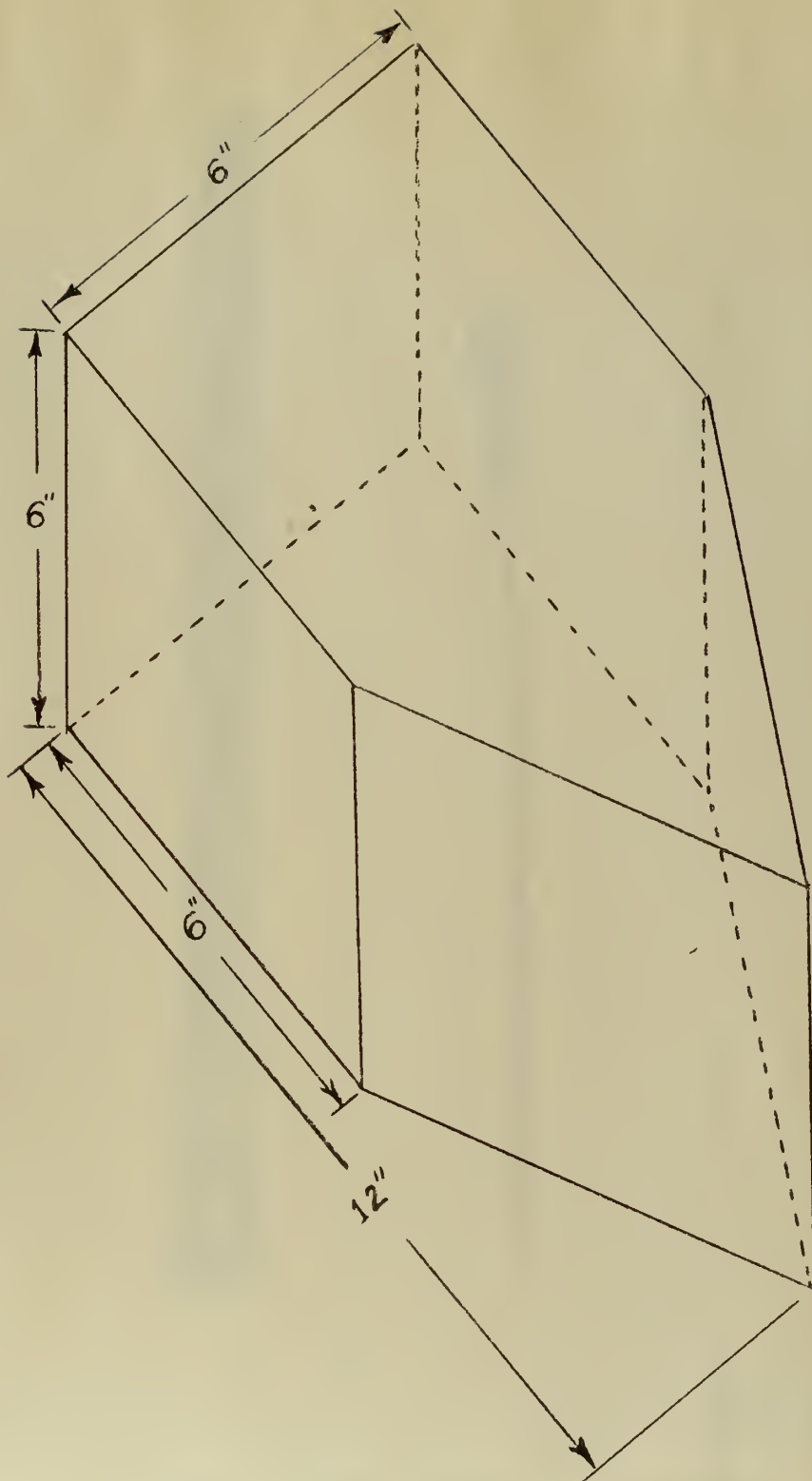


Figure 3. Isometric view of sound absorbing wedge.



FIGURE 4. SOUND SOURCE (LEFT) AND RECEIVER.

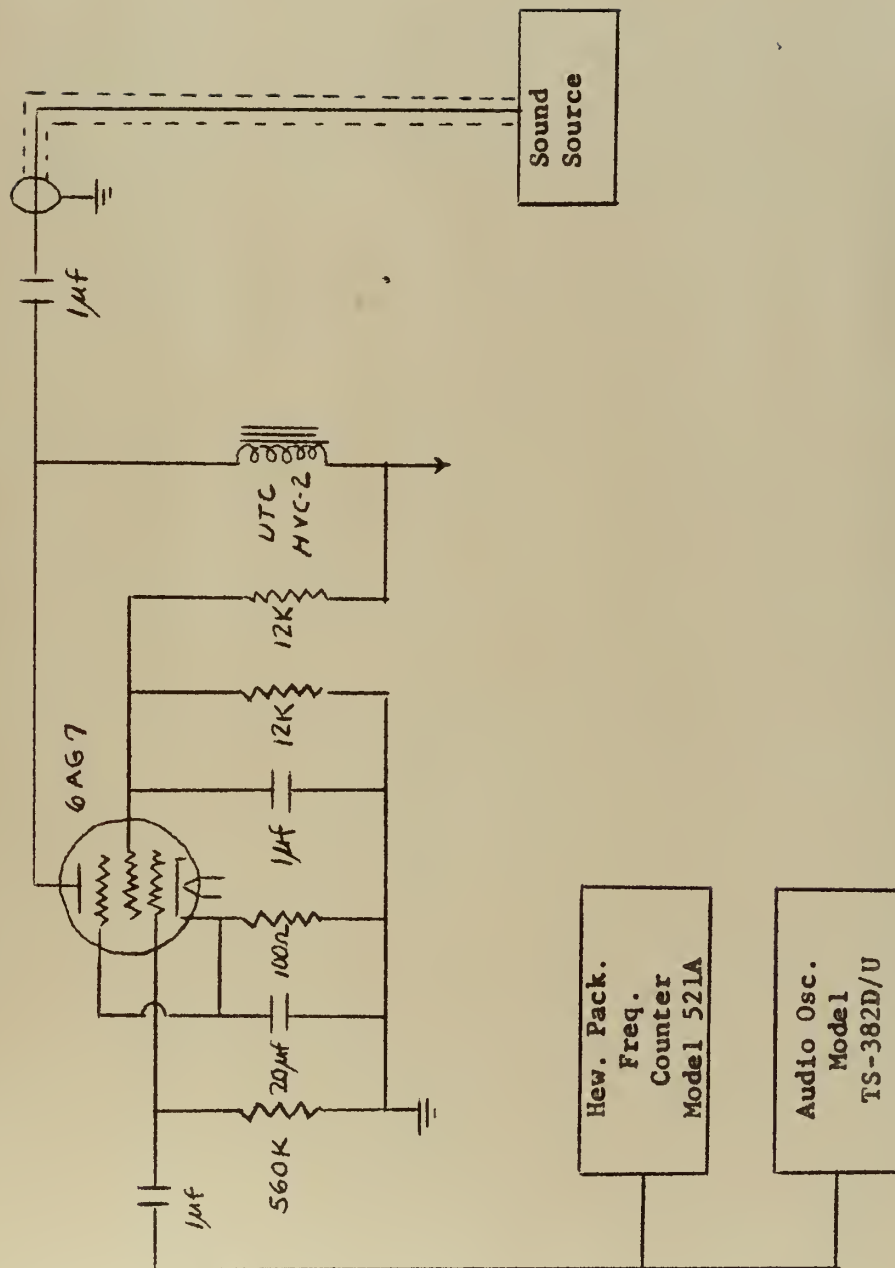


Figure 5 - Diagram of Sound Source Electronic Equipment

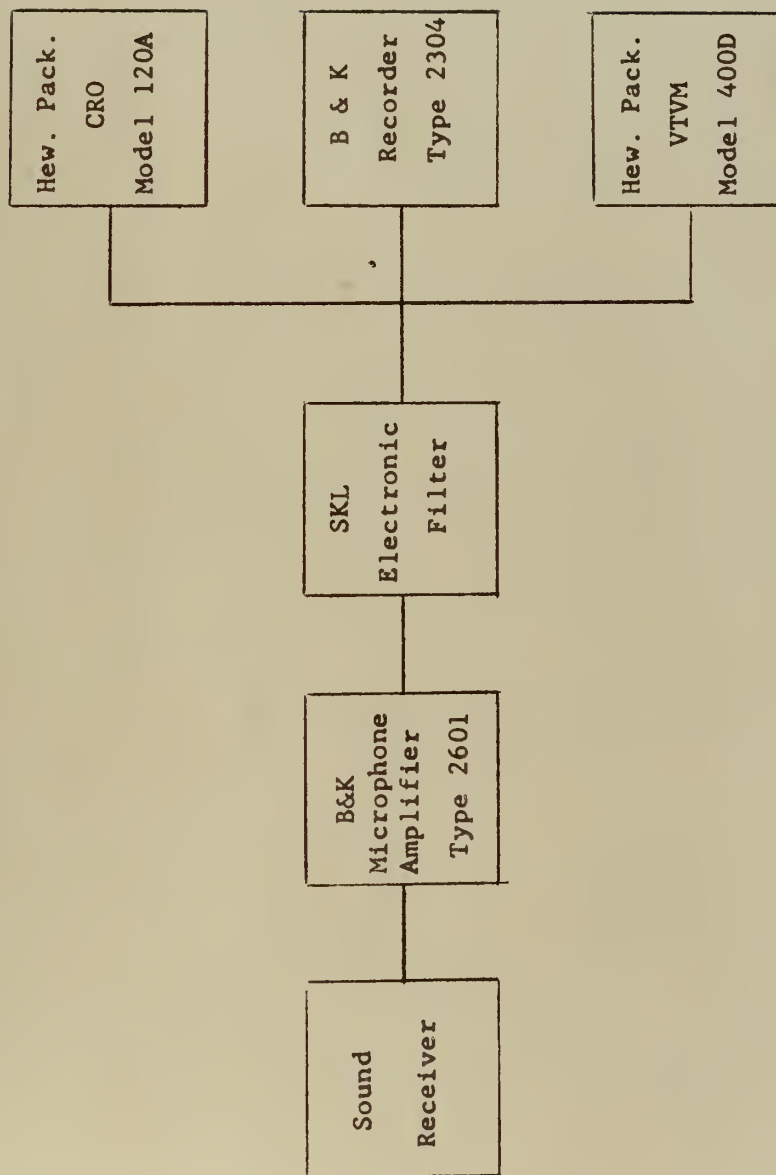


Figure 6 - Block Diagram of Sound Source Electronic Equipment

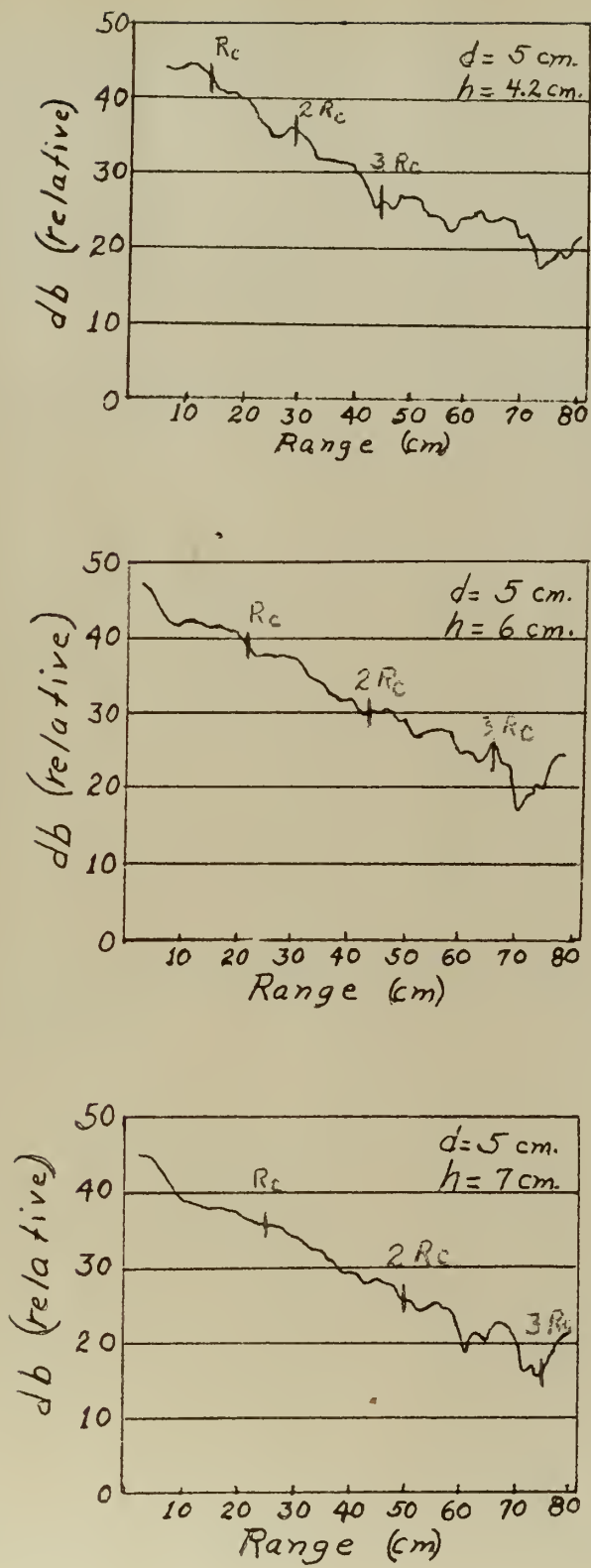


Figure 7. Sound Pressure Patterns showing dron-off from R_c to $3R_c$.

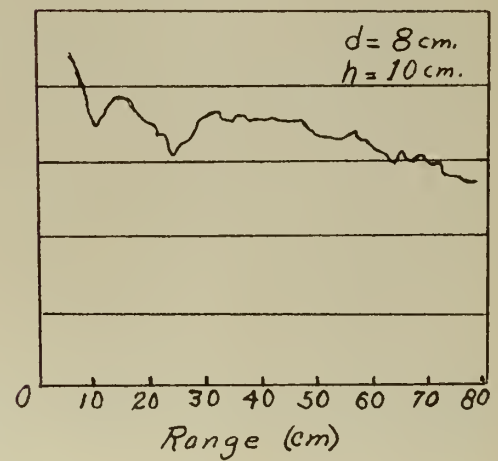
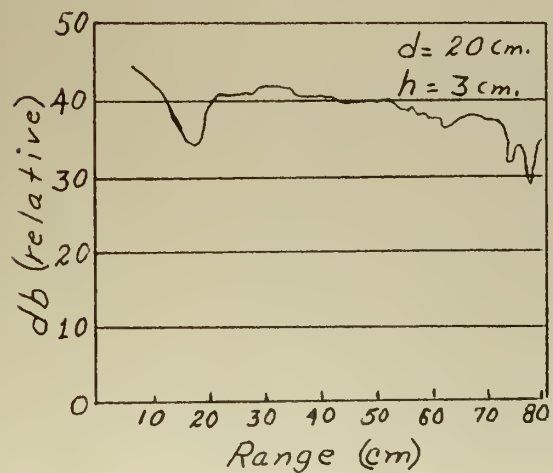
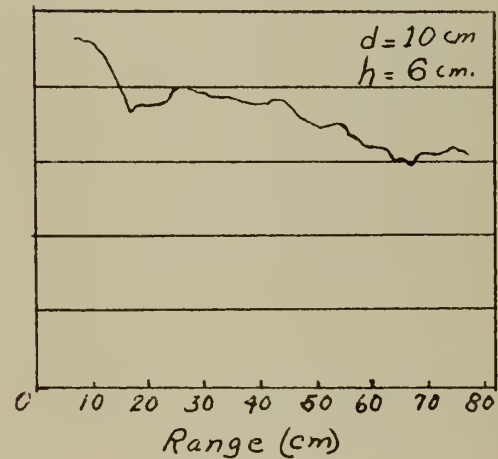
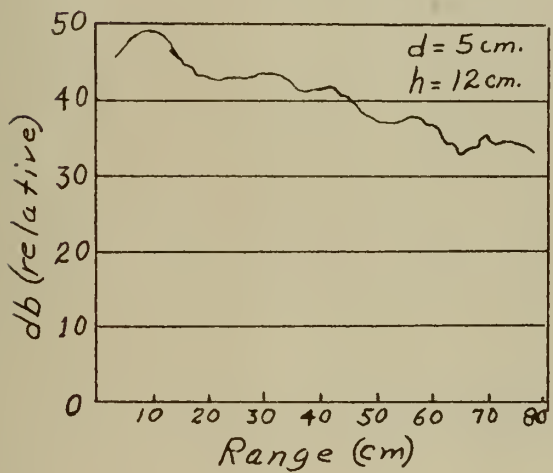
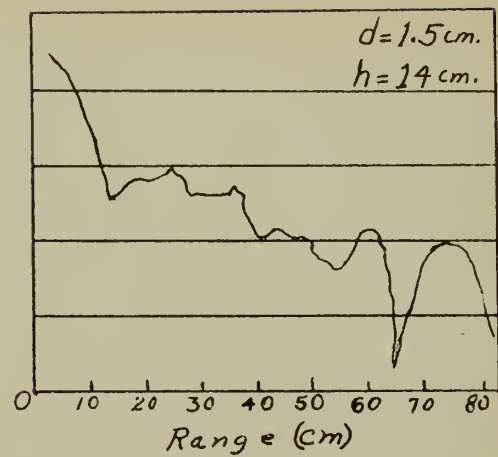
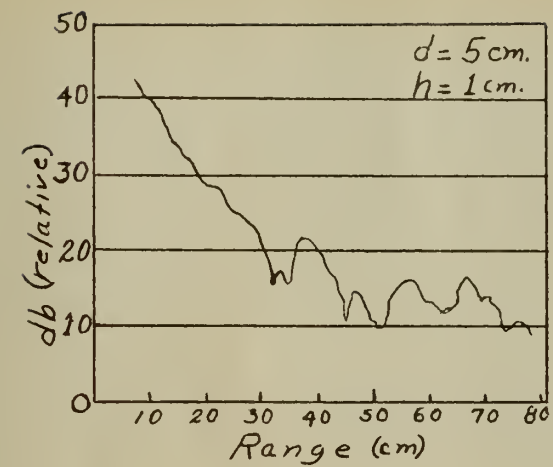


Figure 8. Sound Pressure Patterns showing effect of extremes in source and receiver depths.

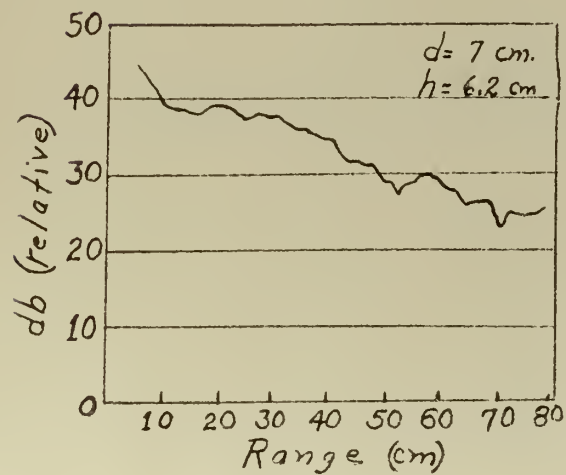
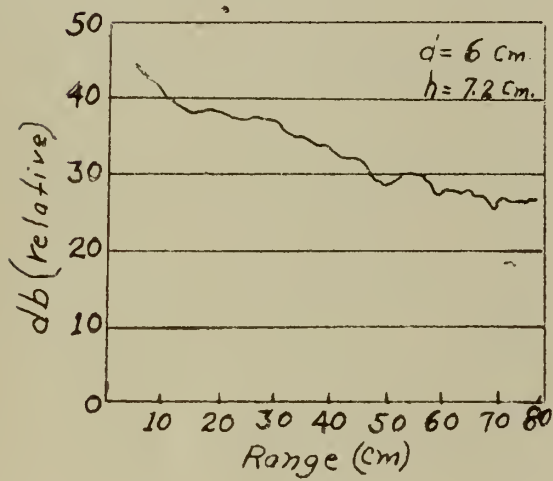
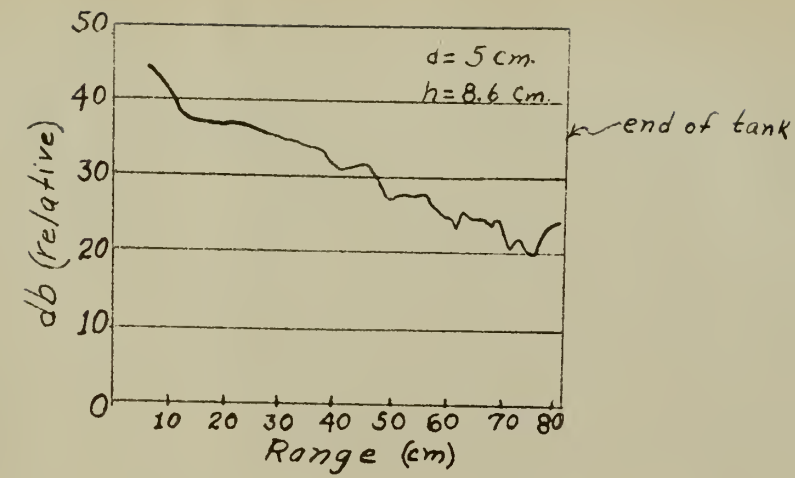


Figure 9. Sound Pressure Patterns with product of h and d constant.

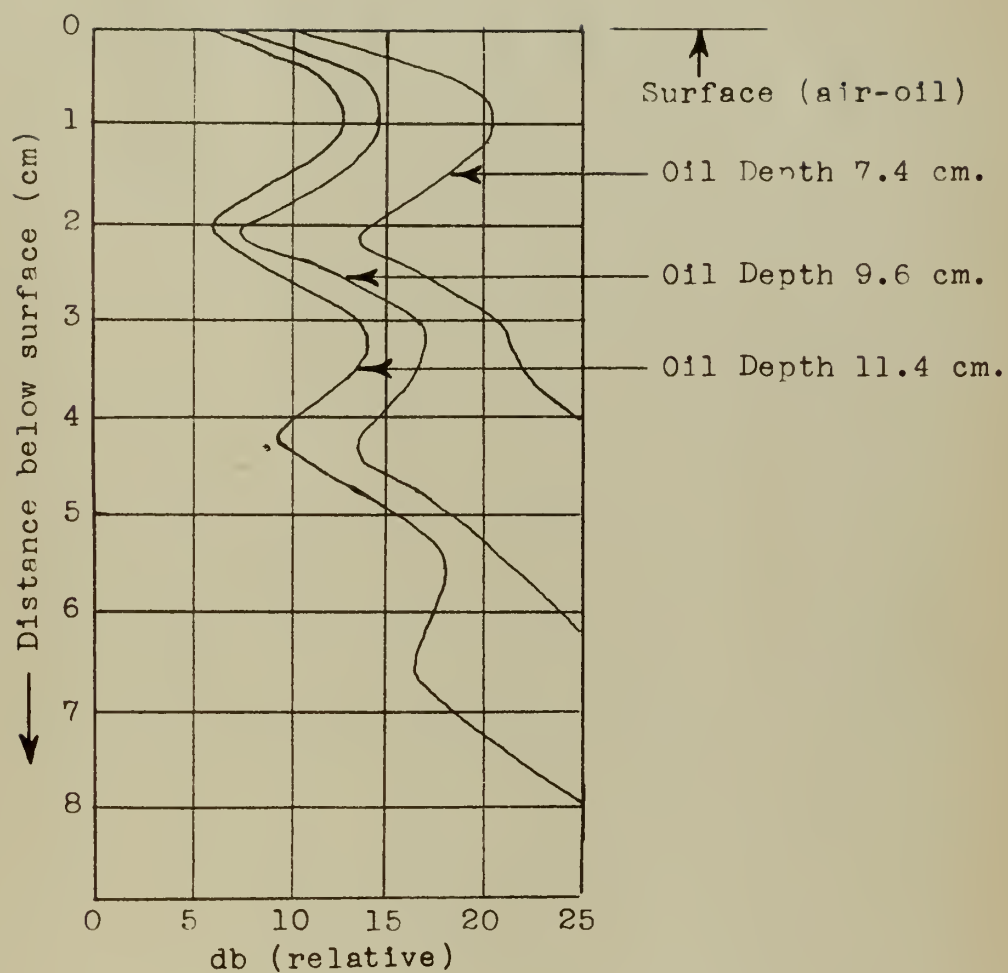


Figure 10. Vertical Sound Pressure Patterns from Surface to Source in the two-layer Model.

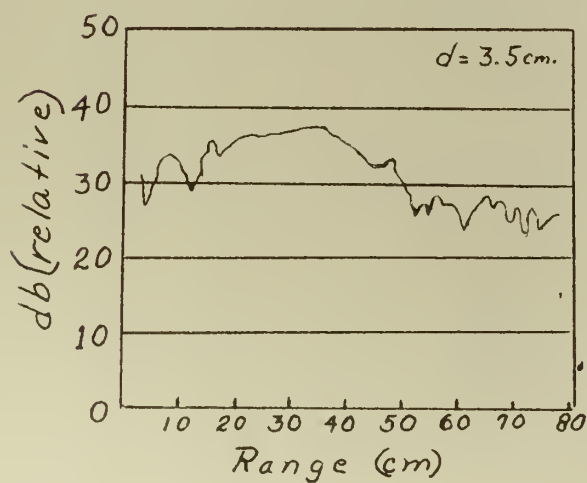
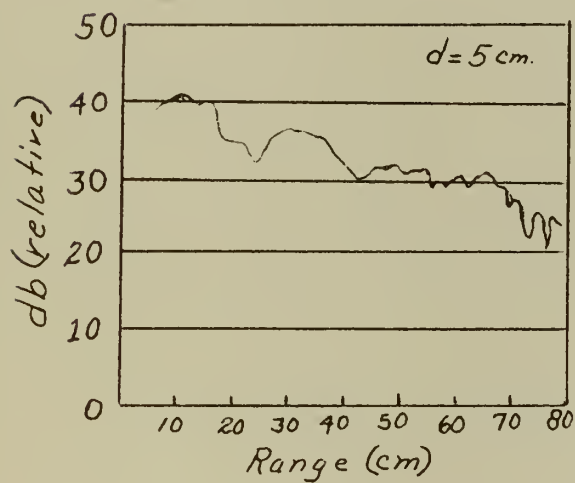
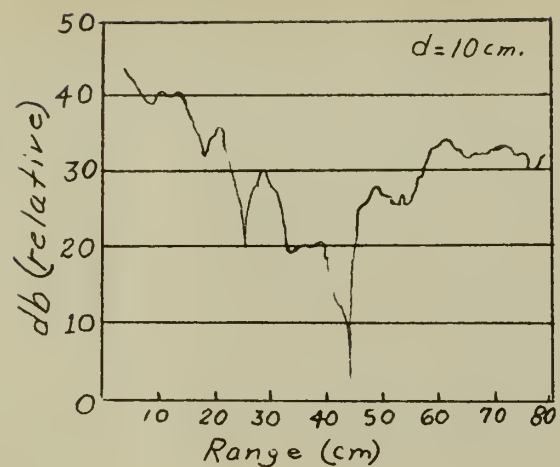


Figure 11. Sound Pressure Patterns Along the Bottom of the Oil Layer at Various Source Depths " d ." Layer Depth 11.4 cm.

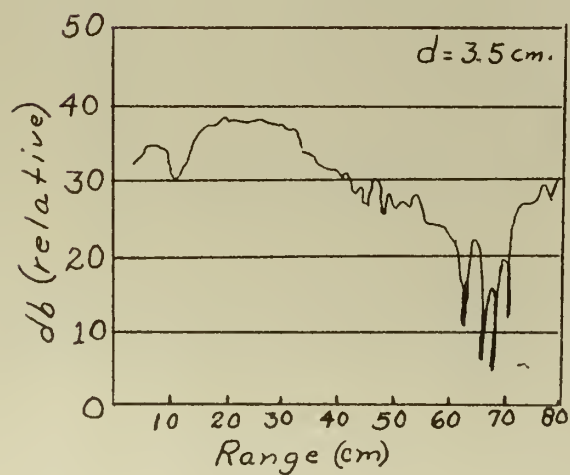
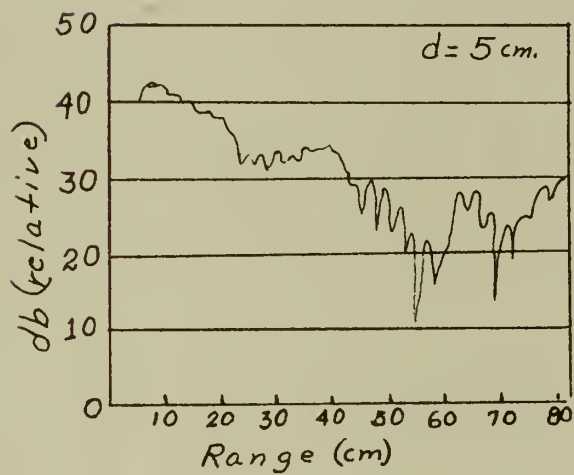
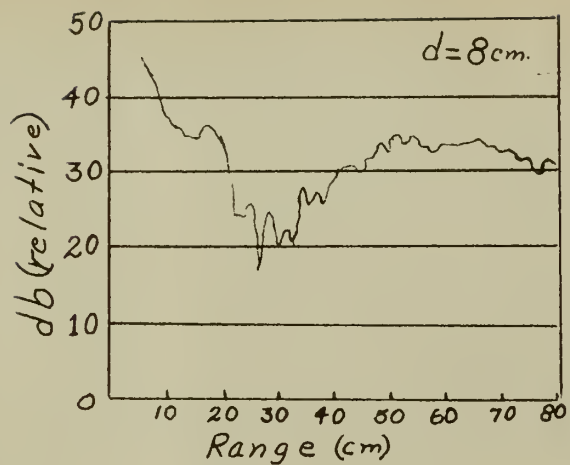


Figure 12. Sound Pressure Patterns Along the Bottom of the Oil Layer at Various Source Depths " d ." Layer Depth 9.6 cm.

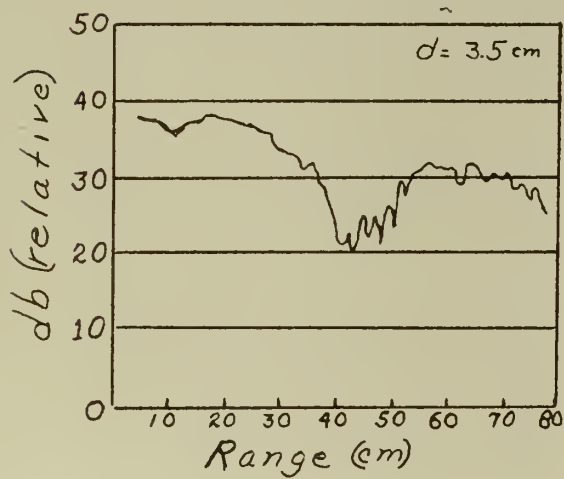
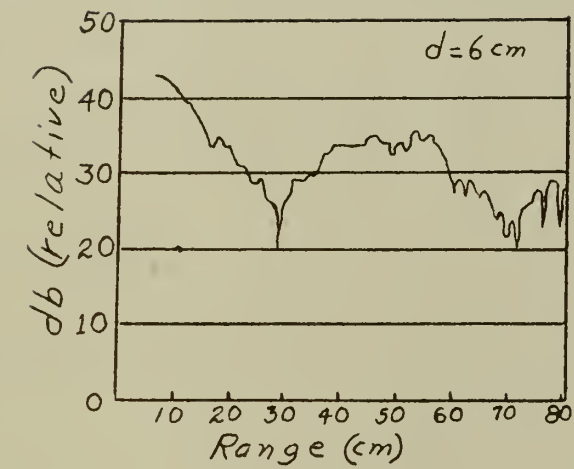


Figure 13. Sound Pressure Patterns Along the Bottom of the Oil Layer at Different Source Depths " d ." Layer Depth 7.5 cm.

BIBLIOGRAPHY

1. C. L. Pekeris, Theory of Propagation of Explosive Sound in Shallow Water, Geological Society of America, Memoir 27, 1948.
2. M. S. Weinstein, Short Range Propagation of Sound in Shallow Water, NAVORD Report 4373, 1956.
3. A. R. Yingling, Jr. and H. Medwin, A Lloyd's Mirror Test of a Wedge-Lined Anechoic Tank, The Journal of the Acoustical Society of America, Vol. 31, p. 131, January 1959.
4. C. L. Darner, An Anechoic Tank for Underwater Sound Measurements Under High Hydrostatic Pressure, The Journal of the Acoustical Society of America, Vol. 26, March 1954.
5. E. G. Richardson, Technical Aspects of Sound, Vol. II, Elsevier Publishing Co., 1957.
6. R. A. Langevin, The Electro-Acoustic Sensitivity of Cylindrical Ceramic Tubes, The Journal of the Acoustical Society of America, Vol. 26, May 1954.
7. L. E. Kinsler and A. R. Frey, Fundamentals of Acoustics, John Wiley & Sons, 1950.
8. V. A. Del Grosso and E. J. Smura, Naval Research Laboratory Report 4191, 18 September 1953.
9. American Institute of Physics Handbook, McGraw-Hill Book Co., Inc. 1957.

APPENDIX I

FLUIDS SUITABLE FOR MODEL STUDIES

The theoretical solution to the problem of sound propagation in shallow water includes the computation of a reflection coefficient for the sea water-bottom interface. This coefficient is a function of the ratio of the specific acoustic impedance of the sea water to that of the bottom material. The ratio may vary between 1:1.5 for a mud or silty fine sand to 1:2.4 for coarse sand. To model these conditions in a test tank it is necessary to select fluids which will produce specific acoustic impedance ratios within the above range. Other desired properties of the fluids are: low water solubility, high fire point, low vapor pressure, low toxicity, high chemical stability, low cost and ready availability.

Del Grosso and Smura [8] investigated acoustic and other physical properties of liquids suitable for sound applications. The acoustic properties of various liquids are tabulated in the American Institute of Physics Handbook [9].

Many of the fluids listed in the above references must be eliminated from consideration since they possess acoustic impedances close to that of sea water. Others, such as the hydrocarbons, have low fire points and are not suitable for use near electrical equipment. In summary, there are no fluids that possess all of the desired properties. However, the following should be considered:

	Velocity at 20° C. (cm/sec x 10 ⁻⁵)	Density at 20° C. (gm/cm ³)	Specific Acoustic Impedance at 20° C. (gm/sec cm ² x 10 ⁻⁵)
Butyl Chloride	1.14	0.88	1.01
Orsil BF -1	1.30	0.88	1.14
Transformer Oil	1.42	0.86	1.23
Brine (35g/100ml)	1.72	1.20	2.06
Glycerine (5% H ₂ O)	1.92	1.23	2.36

Proper selection of these fluids will give specific acoustic impedance ratios within the desired range. With the exception of Butyl Chloride, all are safe for use near electrical equipment. Butyl Chloride should not be used unless facilities are such that fire hazards may be tolerated.

thesT42

An anechoic tank for underwater sound st



3 2768 002 03493 6

DUDLEY KNOX LIBRARY